Co_3O_4-Bi_2O_3 heterojunction; An effective photocatalyst for photodegradation of rhodamine B dye

Muhammad Saeed (msaeed@gcuf.edu.pk)
Government College University Faisalabad https://orcid.org/0000-0002-8759-6948
Afifa Baig
Government College University Faisalabad
Muhammad Asghar Jamal
Government College University Faisalabad
Nadia Akram
Government College University Faisalabad
Tanveer Hussain Bokhari
Government College University Faisalabad

Research Article

Keywords: Co3O4-Bi2O3, Heterojunction, Photodegradation, Rhodamine B, Kinetics analysis

Posted Date: April 26th, 2021

DOI: https://doi.org/10.21203/rs.3.rs-463319/v1

Version of Record: A version of this preprint was published at Arabian Journal of Chemistry on January 1st, 2022. See the published version at https://doi.org/10.1016/j.arabjc.2022.103732.

Abstract

Recently, the research on development of visible-light-active photocatalysts for photodegradation of organic pollutants has got much attention. Therefore, this study reports the synthesis of Co_3O_4-Bi_2O_3 heterojunction as visible-light responsive photocatalyst for photodegradation of rhodamine B dye. The Co_3O_4-Bi_2O_3 heterojunction was synthesized by coprecipitation method and characterized by XRD, EDS, SEM, TGA and FTIR. The as prepared Co_3O_4-Bi_2O_3 heterojunction was utilized as photocatalyst for photodegradation of rhodamine B dye using a 100 mg/L solution. It was observed that Co_3O_4-Bi_2O_3 showed best catalytic performance with ~ 92% degradation of rhodamine B dye than Co_3O_4 and Bi_2O_3 with 14 and 34% removal of rhodamine B dye, respectively. The rate constant for Co_3O_4-Bi_2O_3 catalyzed photodegradation of rhodamine B was 6 times and 3 times higher than rate constant for Co_3O_4 catalyzed and Bi_2O_3 catalyzed photodegradation of rhodamine B, respectively. The pH 8 was found as optimum pH for Co_3O_4-Bi_2O_3 catalyzed photodegradation of rhodamine B dye.

1 Introduction

The removal of organic pollutants from aqueous system by photocatalysis employing semiconductor metal oxides as photocatalysts plays a crucial role in treatment of wastewater due to its advantages of mild reaction conditions, complete mineralization of pollutants and low processing cost (Chen et al. 2018a) (Meng et al. 2019). An ideal photocatalyst for photodegradation of organic pollutants is the one which can effectively degrade the pollutants under irradiation of visible light. A narrow band gap semiconductor can be used as photocatalyst under irradiation of visible light, however the fast recombination of photo induced positive holes and electrons inhibits the photocatalytic activity (Huang et al. 2017) (Zhong et al. 2017). Therefore, attempts are made to inhibit the recombination of photo induced positive holes and electrons by developing the composite materials. In this respect, a number of studies have been reported for the synthesis of active visible-light photocatalysts for the treatment of wastewater contaminated with organic pollutants (Gan et al. 2018). The development of visible light responsive active photocatalyst for dyes contaminated wastewater is a hot topic among the researchers of photocatalysis.

The semiconductor bismuth oxide, Bi_2O_3, has recently attracted the interest of researchers due to suitable price, stable structure, and suitable band gap energies. The bismuth oxide, Bi_2O_3, exists in different crystal types: the α-Bi_2O_3, β-Bi_2O_3, γ-Bi_2O_3, δ-Bi_2O_3, ε- Bi_2O_3 and ω-Bi_2O_3 (Zhang et al. 2018) (Ho et al. 2013). Among different crystal types, the α-Bi_2O_3, β-Bi_2O_3 have been widely used in catalysis, chemical sensors, fuel cells, photovoltaic cells, and optical thin films. The α-Bi_2O_3 and β-Bi_2O_3 has band gap of 2.85 and 2.58 eV respectively, hence both can be activated under visible irradiation (Chen et al. 2018b) (Song et al. 2020). However, the fast recombination photoinduced electron-hole limits the practical application of Bi_2O_3 as visible light photocatalyst. Therefore, attempts have been made to reduce the rate of recombination of photoinduced electron-hole. The coupling of Bi_2O_3 with semiconductors is one of the

effective ways to separate the photoinduced electron and hole. The coupling of Bi_2O_3 with a semiconductor metal oxide results in formation of a heterojunction interface with an electric field between two semiconductors. In this way, the electric field created at the heterojunction assists the transport of charges from one semiconductor to other resulting an effective separation between the photoinduced charges (Balachandran and Swaminathan 2012). Hence in Bi_2O_3-semiconductor heterojunctions, advantages such as separation of charges, increased lifetime of charges and enhanced transfer efficiency of the charges to adsorbed substrate can be achieved. In this study, the development of heterojunction formed by coupling of Bi_2O_3 with spinel cobalt tetroxide (Co_3O_4) is reported. The spinel cobalt oxide (Co_3O_4) which composed of Co (II) and Co (III) has been studied extensively due to its extra ordinary properties. The high catalytic activity of Co_3O_4 is thought to be due to adsorption of oxygen in different states, oxygen defects and variance in oxygen holes in Co_3O_4. Furthermore, the narrow band gap in the range of 1.2–2.1 eV makes Co_3O_4 attractive in photocatalysis for treatment of wastewater contaminated with organic pollutants (Malefane 2020) (Hu et al. 2019) (Luo et al. 2019) (Zhao et al. 2019) (Rao and Sunandana 2008). As Bi_2O_3 has oxygen vacancies in its crystals, and Co_3O_4 is rich with oxygen content, therefore Bi_2O_3 promote mobility and activity of lattice oxygen in Co_3O_4 which results in separation of photoinduced electron-hole pair and ultimately enhances the photo catalytic activity.

2 Experimental

2.1 Synthesis of photocatalyst

The Co_3O_4-Bi_2O_3 hetero-structure was prepared by coprecipitation method. Typically, 12.5 mmol of cobalt nitrate hexahydrate and 12.5 mmol of bismuth nitrate pentahydrate were dissolved in 10 mL (1M) nitric acid solution under vigorous stirring. Then, 1M of sodium hydroxide solution was added dropwise to above mixed solution under continuous stirring at 60°C till pH 12 obtained. The solution was further stirred for 2 h at 60^oC. As a result, a green precipitate was formed. The resultant precipitate was filtered, washed with ethanol, and distilled water till all unreacted ions were eliminated from prepared precipitate. Then, the washed precipitate was dried at 100^oC overnight. Finally, the dried residue was calcined at 500^oC for 3 hours which resulted black colored Co_3O_4-Bi_2O_3 hetero-structure.

For comparison, Co_3O_4 and Bi_2O_3 were also prepared. The Co_3O_4 was prepared as follows. A 100 mL solution of cobalt nitrate hexahydrate (0.03M) was mixed with a 100 mL solution of potassium carbonate (0.06M) under sitting. The resultant reaction mixture was stirred for 7 hours at 70°C. the obtained residue was filtered, washed, and dried at 100°C for 12 hours. Finally, the dried sample was calcined at 500°C for 3 hours to get Co_3O_4 particles.

The Bi_2O_3 was prepared by adding 1M sodium hydroxide solution to a solution containing 4.85g bismuth nitrate pentahydrate in 100 mL till pH 12 obtained. Concentrated nitic acid was used for dissolution of bismuth nitrate. The resultant precipitate was filtered, washed, and dried at 100°C for 12 hours. The dried product was calcined at 500°C to get light yellow Bi_2O_3 particles

2.2 Characterization

X-rays diffraction, energy dispersive spectroscopy, scanning electron microscopy, thermal gravimetric analysis and infrared spectroscopy were used for characterization of prepared material using JOEL-JDX-3532 Japan X-ray diffractometer, JEOL-JSM 5910 Japan Scanning electron microscope, JSM5910 UK Energy dispersive X-rays spectrophotometer, Perkin Elmer 6300 TGA analyzer and Bruker VRTEX70 Infrared spectrophotometer, respectively.

2.3 Catalytic activity

The photo-catalytic activities of synthesized particles were determined with photo degradation of rhodamine B dye. Typically, a solution of rhodamine B dye was charged with a predetermined catalyst dose and stirred under visible irradiation for 120 minutes. Progress of photo catalytic degradation was monitored by sampling and analyzing the reaction mixture at regular time interval. Blank experiments were performed by stirring the dye solution and dye solution with catalyst under irradiation and dark conditions, respectively. UV/Vis spectrophotometer (U-2800, HITACHI, Japan) was used for measurement of photocatalytic activity.

3 Results And Discussion

3.1 Characterization

The formation of Co_3O_4, Bi_2O_3 and Co_3O_4-Bi_2O_3 were confirmed by XRD analysis. The XRD of Co_3O_4 given in Fig. 1a consists of sharp diffraction peaks which show the crystalline nature of Co_3O_4. The diffraction peaks observed at 2θ ~ 18, 30, 37, 43 and 58° have been indexed to spinel structure of Co_3O_4 (Manickam et al. 2016) (Rao and Sunandana 2008) (R. Manigandan, K. Giribabu, R. Suresh, L. Vijayalakshmi, A. Stephen 2013). Similarly, the diffraction peaks at 2θ ~ 12, 26, 33, 36, 41, 46, 54 and 58 are observed in XRD of Bi_2O_3. All these diffraction peaks correspond to β-Bi_2O_3. The remaining weak diffraction peaks in XRD of Bi_2O_3 represent the γ-Bi_2O_3. Hence, it is concluded that Bi_2O_3 is composed of mixed phases of β-Bi_2O_3 and γ-Bi_2O_3 crystals, however the β-Bi_2O_3 is the main constituent in crystalline phase (Iyyapushpam et al. 2015) (Liang et al. 2014) (Huang et al. 2016).

The elemental composition of as-prepared material was investigated by energy dispersive spectroscopy using JSM5910, INCA200 UK. Figure 2 shows the energy dispersive spectra of the samples. The energy dispersive spectrum of Co_3O_4 given in Fig. 2a shows peaks for Co and O only which confirms the purity of the sample. The EDS analysis showed that prepared cobalt oxide is composed of 87.3 weight% Co and 12.68 weight% O. The energy dispersive spectrum of bismuth oxide (Fig. 2b) shows peaks for Bi, O and C. The EDS analysis showed that prepared bismuth oxide is composed 58.08, 9.97 and 4.95% Bi, O and C respectively. The existence of C may be due to impurities in precursor material. Similarly, the energy dispersive spectrum of cobalt oxide-bismuth oxide composite (Fig. 2c) shows that the composite is composed of 11.6, 70.83, 13.92 and 4.19% Co, Bi, O and C respectively.

The morphology of Co_3O_4, Bi_2O_3 and Bi_2O_3-Co_3O_4 was studied by scanning electron microscopy with JEOL-JSM-5910, Japan scanning electron microscope. JEOL-JSM-420, Japan coating machine was used for mounting and coating the samples with gold foil. The scanning electron micrographs given in Fig. 3 show that the particles of as-prepared samples are irregular in shape, non-agglomerated and dispersed. The non-agglomerated and dispersed particles have enhanced catalytic activity as the active centers are easily accessible to substrate molecules.

Thermal stability of as prepared samples was estimated by thermal gravimetric analysis using Perkin Elmer 6300 TGA analyzer. As given in Fig. 4, there was only about 5% loss in weight of the samples up to 700°C, which is attributed to loss of moisture content. The non-significant weight loss shows the stability of as prepared samples over a wide range of temperature.

The typical bonds and functional groups of as prepared samples were estimated by Fourier transform infrared spectroscopy (FTIR) using Bruker (VRTEX70 series). Figure 5 shows the FTIR spectra of as-prepared samples in which several peaks can be observed. The absorption peak at 1634 cm^{-1} is attributed to -OH groups present at the surface of Co_3O_4-Bi_2O_3 heterojunction. The absorption bands at ~ 445 cm^{-1} and 846 cm^{-1} have been assigned to stretching vibrations of Bi-O and Bi-O-Bi bonds, respectively. The absorption bands at ~ 571 and 668 are representative peaks of Co_3O_4 due to Co-O stretching vibrations (Tang et al. 2018) (Hammad et al. 2016) (Li et al. 2017) (M. Ilyas 2010) (Saeed et al. 2012). The FTIR result show the successful formation of Co_3O_4-Bi_2O_3 heterojunction.

3.2 Catalytic activity

The photocatalytic activity of Co_3O_4, Bi_2O_3 and Co_3O_4-Bi_2O_3 was evaluated by performing photodegradation experiments of rhodamine B dye in the presence of 0.05g of afore mentioned catalysts under visible irradiation. A 50 mL rhodamine B (100 mg/L) was taken in Pyrex glass beaker and was stirred under irradiation for 30 minutes. Then, as blank reaction, 0.05g Co_3O_4/Bi_2O_3/Co_3O_4-Bi_2O_3 was added to dye solution and stirred for 30 minutes under dark to clarify the effect of adsorption. For evaluation of catalytic performance, the reaction mixture, was then irradiation under stirring. The change in concentration of rhodamine B due to catalytic degradation was monitored by measurement of absorbance at wavelength 554 nm using UV-visible spectrophotometer. As the normalized temporal changes in absorbance (A_t/A_o) of rhodamine B is during photocatalytic process are proportional to normalized concentrations (C_t/C_o) of rhodamine B dye, therefore, the photocatalytic activity was expressed as A_t/A_o vs t as given in Fig. 6 (A_t: absorbance of rhodamine B at time t, A_o; Initial absorbance of rhodamine B, C_t: concentration of rhodamine B at time t, C_o: initial concentration of rhodamine B). It was observed that Co_3O_4-Bi_2O_3 showed best catalytic performance with ~ 92% degradation of rhodamine B dye than Co_3O_4 and Bi_2O_3 with 14 and 34% removal of rhodamine B dye, respectively. The obtained results show that coupling of Co_3O_4 with Bi_2O_3 significantly promotes the catalytic activity.

Leaching experiment was also performed to confirm whether the photodegradation of rhodamine B is heterogeneous or homogeneous reaction. For this purpose, 0.1g Co_3O_4-Bi_2O_3 was suspended in 50 mL

distilled water and stirred under irradiation for 120 minutes. Then, the Co_3O_4-Bi_2O_3 was filtered and a known solution of rhodamine B was added to filtrate to get a ~ 100 mg/L dye solution and analyzed with UV-visible spectrophotometer. Finally, the dye solution was again treated with irradiation and analyzed with UV-visible spectrophotometer after 120 minutes. The analysis showed that there was no change in concentration of the dye. Hence, it is concluded that Co_3O_4-Bi_2O_3 does not leach to aqueous medium in this study.

Co_3O_4-Bi_2O_3 is a second generation photocatalyst. The second generation photocatalysts, also called as heterojunctions were developed to overcome the drawback of first generation photocatalysts (Anwer et al. 2019). The single component metal oxides are classified as first generation photocatalysts. The fast recombination of electron-hole is a basic drawback of first generation photocatalysts. In second generation photocatalysts, the photoinduced electrons are confined in conduction band of one component of heterojunction while the holes are confined in valence band of the other component. This spatial separation of the photoinduced electrons and holes inhibits their recombination. As a result, active cites are generated at which degradation of organic pollutants takes place. The second-generation photocatalytic materials show light absorbance in the visible region ($\lambda \geq 420$ nm) accompanied with lower band gap energies than first generation photocatalytic materials. Hence, the photodegradation of rhodamine B dye in present study can be described as follow.

$$Co_3O_4 - Bi_2O_3 + Visible\ irradiation \rightarrow h^+(Co_3O_4 - Bi_2O_3) + e^-(Co_3O_4 - Bi_2O_3) \quad (1)$$

$$h^+(Co_3O_4 - Bi_2O_3) + H_2O \rightarrow OH \quad (2)$$

$$e^-(Co_3O_4 - Bi_2O_3) + (O_2)_{ads} \rightarrow \rightarrow OH \quad (3)$$

$$[RH] + OH \rightarrow Degradation\ products \quad (4)$$

The photoinduced electron, positive hole and OH radicals are the active species which contribute to photodegradation of rhodamine B dye. The role played by these species was confirmed by scavenging experiments. For this purpose, EDTA and BQ were separately used as scavengers each of which significantly suppressed the photodegradation activity. Since, the EDTA arrests the positive holes, therefore the activity decreased in the presence of EDTA. Similarly, the addition of BQ suppress the photodegradation because it reacts with super oxide anion radicals (Song et al. 2020) (Xu et al. 2019).

Based on above mechanism, the rate expression is written as

$$-\frac{d[RH]}{dt} = k\,(O_2)_{ads}\,[RH]^n \quad (5)$$

$$-\frac{d[RH]}{dt} = k_{obs}\,[RH]^n \quad (6)$$

$$ln\frac{A_o}{A_t} = k_1\,t \quad (7) \quad (\text{For n} = 1)$$

$$\frac{1}{A_t} = \frac{1}{A_o} + k_2\,t \quad (8) \quad (\text{For n} = 2)$$

k_{obs}, k_1, k_2, A_o and A_t is observed rate constant, 1st order rate constant, 2nd order rate constant, initial absorbance of rhodamine B and absorbance at time t respectively.

Figure 7 shows the kinetics treatment of the photodegradation degradation data of rhodamine B. The 1st order rate constant (k_1) and 2nd order rate constant (k_2) are given in Table 1. As the regression coefficient (R^2) values are higher for 1st order kinetics treatment, therefore, it proposed that the degradation of rhodamine B dye in this study follows 1st order reaction kinetics. The rate constant for Co_3O_4-Bi_2O_3 catalyzed photodegradation of rhodamine B was 6 times and 3 times higher than rate constant for Co_3O_4 catalyzed and Bi_2O_3 catalyzed photodegradation of rhodamine B respectively. Hence, the formation of Co_3O_4-Bi_2O_3 heterostructure significantly boosts up the catalytic performance of Co_3O_4 and Bi_2O_3.

Table 1 The 1st order and 2nd order rate constants for photodegradation of rhodamine B

Catalyst	$ln\frac{A_o}{A_t} = k_1\,t$		$\frac{1}{A_t} = \frac{1}{A_o} + k_2\,t$		*Catalytic efficiency (%)
	k_1	R^2	k_2	R^2	
Co_3O_4	0.0015	0.994	0.006	0.975	14
Bi_2O_3	0.003	0.977	0.0137	0.951	34
Co_3O_4-Bi_2O_3	0.0089	0.988	0.0541	0.879	92
*Reaction duration: 120 minutes					

3.3 Effect of pH

The pH of solution significantly affects the catalytic activity; therefore, the pH was optimized as well in this study. The effect of pH on catalytic activity of Co_3O_4-Bi_2O_3 was evaluated by performing degradation

experiment at pH 4, 6, 8 and 10. Figure 8 shows the effect of pH on photocatalytic degradation of rhodamine B dye (the numbers given at bar graphs represent the catalytic efficiency). Every experimental cycle was performed with a 0.05g Co_3O_4-Bi_2O_3 per 50 mL solution (100 mg/L). The reaction duration was 60 minutes. It was observed that increase in pH up to 8 favored the catalytic activity. The point of zero charge (PZC) for Co_3O_4-Bi_2O_3 has been reported as pH 8.4 (Ivanova-Kolcheva et al. 2020), hence the surface of Co_3O_4-Bi_2O_3 becomes negative at pH higher than PZC and positive at pH lower than PZC. At pH lower than PZC, both the rhodamine B and surface of the Co_3O_4-Bi_2O_3 are positive, therefore the catalytic activity is low at low pH due to electrostatic repulsion. Similarly, the negative surface of Co_3O_4-Bi_2O_3 at higher pH also opposes the adsorption of rhodamine B, hence the maximum catalytic activity exhibited at pH 8.

3.4 Effect of catalyst dose

The dependance of photocatalytic activity of Co_3O_4-Bi_2O_3 towards photodegradation of rhodamine B on photocatalyst dosage has been investigated by performing photodegradation experiments with different dosage of Co_3O_4-Bi_2O_3 under identical condition. In a model experiment, a 50 mL solution of rhodamine B dye (100 mg/L) was treated with a known amount of Co_3O_4-Bi_2O_3 for 60 minutes. Figure 9 shows the dependance of catalytic activity on catalyst dosage. It was observed that increase in catalyst dose from 0.01 to 0.05g increased the degradation from 18 to 36%, however further increase in catalyst dose caused a decreased in degradation efficiency. The enhancement in catalytic efficiency with increase in catalyst dose is due to two reasons: (1) The number of molecules of rhodamine B adsorbed increases with catalyst dosage, (2) the density of Co_3O_4-Bi_2O_3 particles under illumination increases with catalyst dosage. The decrease in catalytic efficiency at higher catalyst dosage is due to scattering of light. Hence, a catalyst dose of 0.05g/50 mL of dye solution is found to be optimum catalyst dosage in this study.

3.5 Effect of concentration

The initial concentration of dye also affects the catalytic activity, therefore the concentration dependance of catalytic activity has been also investigated. This investigation was carried out by performing separate photodegradation experiments of rhodamine B dye in the presence of 0.05g Co_3O_4-Bi_2O_3 using 100, 200 and 300 mg/L solutions of rhodamine B dye. Figure 10a shows the effect of concentration on catalytic activity Co_3O_4-Bi_2O_3 towards photodegradation of rhodamine B dye. It was found that catalytic activity decreased with increase in initial concentration of rhodamine B dye. The decrease in catalytic activity with increase in concentration of dye is due to three reasons (Balcha et al. 2016) (Saeed et al. 2017) (Nisar et al. 2021) (Adeel et al. 2021):

1. The pathlength of photon decreases with increase in concentration of dye
2. The rhodamine B dye absorbs photons significantly than catalyst at higher concentration of dye
3. The ration of OH radicals to rhodamine B molecules decreases with increase in concentration

The degradation data given in Fig. 10a was analyzed for kinetics studies using kinetics Eq. 7. Figure 10b shows the fitting of 1st order kinetics model (Eq. 7) to experimental data. The kinetics parameters given

in Table 2 shows that rate constant decreases with increase in initial concentration of rhodamine B dye.

Table 2 Kinetics parameters for Co_3O_4-Bi_2O_3 catalyzed photodegradation of rhodamine B

Parameter	100 mg/L	200 mg/L	300 mg/L
k_1 (min^{-1})	0.0089	0.0056	0.0039
R^2	0.988	0.969	0.948
*Catalytic efficiency (%)	92	72	50
*Reaction duration: 120 minutes			

Conclusions

Herein, we prepared the Co_3O_4-Bi_2O_3 heterojunction as visible-light responsive photocatalyst by coprecipitation method for photodegradation of rhodamine B dye successfully. The Co_3O_4-Bi_2O_3 heterojunction was characterized by XRD, EDS, SEM, TGA and FTIR. The as prepared Co_3O_4-Bi_2O_3 heterojunction was utilized as photocatalyst for photodegradation of rhodamine B dye using a 100 mg/L solution. The photocatalytic activity of Co_3O_4-Bi_2O_3, Co_3O_4 and Bi_2O_3 towards photodegradation of rhodamine B dye was found as 92, 14 and 34%, respectively. The 1^{st} order and 2^{nd} order kinetics models were applied to the data of photocatalytic degradation of rhodamine b dye. the effect of pH, catalyst dose and initial concentration of rhodamine B dye on photocatalytic performance was investigated. The Co_3O_4-Bi_2O_3 heterojunction was found as an efficient visible light-driven photocatalyst for photodegradation of rhodamine B dye.

Declarations

Ethics approval and consent to participate

Not applicable

Consent for publication

Not applicable

Authors Contributions

Muhammad Saeed is main research supervisor, who has supervised the experimental work and drafted the manuscript.

Afifa Baig is research student who has carried out the experimental work.

Muhammad Asghar Jamal has helped in supervision of experimental work and drafting of manuscript.

Nadia Akram has helped in supervision of experimental work and drafting of manuscript.

Tanveer Hussain Bokhari has helped in drafting of paper.

Funding

Government College University Faisalabad Pakistan provided financial assistance under GCUF-RSP.

Availability of data and materials

Available on request

References

Adeel M, Saeed M, Khan I, et al (2021) Synthesis and Characterization of Co-ZnO and Evaluation of Its Photocatalytic Activity for Photodegradation of Methyl Orange. ACS Omega 6:1426–1435. https://doi.org/10.1021/acsomega.0c05092

Anwer H, Mahmood A, Lee J, et al (2019) Photocatalysts for degradation of dyes in industrial effluents: Opportunities and challenges. Nano Research 12:955–972. https://doi.org/10.1007/s12274-019-2287-0

Balachandran S, Swaminathan M (2012) Facile fabrication of heterostructured Bi2O3-ZnO photocatalyst and its enhanced photocatalytic activity. Journal of Physical Chemistry C 116:26306–26312. https://doi.org/10.1021/jp306874z

Balcha A, Yadav OP, Dey T (2016) Photocatalytic degradation of methylene blue dye by zinc oxide nanoparticles obtained from precipitation and sol-gel methods. Environmental Science and Pollution Research 23:25485–25493. https://doi.org/10.1007/s11356-016-7750-6

Chen M, Chu W, Beiyuan J, Huang Y (2018a) Enhancement of UV-assisted TiO2 degradation of ibuprofen using Fenton hybrid process at circumneutral pH. Chinese Journal of Catalysis 39:701–709. https://doi.org/10.1016/S1872-2067(18)63070-0

Chen M, Yao J, Huang Y, et al (2018b) Enhanced photocatalytic degradation of ciprofloxacin over Bi2O3/(BiO)2CO3 heterojunctions: Efficiency, kinetics, pathways, mechanisms and toxicity evaluation. Chemical Engineering Journal 334:453–461. https://doi.org/10.1016/j.cej.2017.10.064

Gan L, Xu LJ, Qian K, et al (2018) Hydrothermal synthesis of magnetic graphene-BiFeO3 hybrids and their photocatalytic properties. Xinxing Tan Cailiao/New Carbon Materials 33:221–228

Hammad AH, Marzouk MA, ElBatal HA (2016) The Effects of Bi2O3 on Optical, FTIR and Thermal Properties of SrO-B2O3 Glasses. Silicon 8:123–131. https://doi.org/10.1007/s12633-015-9283-x

Ho C-H, Chan C-H, Huang Y-S, et al (2013) The study of optical band edge property of bismuth oxide nanowires α-Bi_2O_3. Optics Express 21:11965. https://doi.org/10.1364/oe.21.011965

Hu L, Zhang G, Liu M, et al (2019) Application of nickel foam-supported Co3O4-Bi2O3 as a heterogeneous catalyst for BPA removal by peroxymonosulfate activation. Science of the Total Environment 647:352–361. https://doi.org/10.1016/j.scitotenv.2018.08.003

Huang X, Zhang W, Tan Y, et al (2016) Facile synthesis of rod-like Bi2O3 nanoparticles as an electrode material for pseudocapacitors. Ceramics International 42:2099–2105. https://doi.org/10.1016/j.ceramint.2015.09.157

Huang Y, Liang Y, Rao Y, et al (2017) Environment-Friendly Carbon Quantum Dots/ZnFe2O4 Photocatalysts: Characterization, Biocompatibility, and Mechanisms for NO Removal. Environmental Science and Technology 51:2924–2933. https://doi.org/10.1021/acs.est.6b04460

Ivanova-Kolcheva V, Sygellou L, Stoyanova M (2020) Enhanced catalytic degradation of acid orange 7 dye by peroxymonosulfate on Co3O4 promoted by Bi2O3. Acta Chimica Slovenica 67:609–621. https://doi.org/10.17344/ACSI.2019.5617

Iyyapushpam S, Nishanthi ST, Padiyan DP (2015) Synthesis of β-Bi2O3 towards the application of photocatalytic degradation of methyl orange and its instability. Journal of Physics and Chemistry of Solids 81:74–78. https://doi.org/10.1016/j.jpcs.2015.02.005

Li R, Zhou D, Luo J, et al (2017) The urchin-like sphere arrays Co3O4 as a bifunctional catalyst for hydrogen evolution reaction and oxygen evolution reaction. Journal of Power Sources 341:250–256. https://doi.org/10.1016/j.jpowsour.2016.10.096

Liang J, Zhu G, Liu P, et al (2014) Synthesis and characterization of Fe-doped β-Bi2O 3 porous microspheres with enhanced visible light photocatalytic activity. Superlattices and Microstructures 72:272–282. https://doi.org/10.1016/j.spmi.2014.05.005

Luo S, Wang R, Yin J, et al (2019) Preparation and dye degradation performances of self-assembled MXene-Co 3 O 4 nanocomposites synthesized via solvothermal approach. ACS Omega 4:3946–3953. https://doi.org/10.1021/acsomega.9b00231

Ilyas MS (2010) Oxidation of benzyl alcohol in liquid phase catalyzed by cobalt oxide,. International Journal of Chemical Reactor Engineering

Malefane ME (2020) Co3O4/Bi4O5I2/Bi5O7I C-Scheme Heterojunction for Degradation of Organic Pollutants by Light-Emitting Diode Irradiation. ACS Omega. https://doi.org/10.1021/acsomega.0c03881

Manickam M, Ponnuswamy V, Sankar C, et al (2016) The Effect of Solution pH on the Properties of Cobalt Oxide Thin Films Prepared by Nebulizer Spray Pyrolysis Technique. International Journal of Thin Films Science and Technology 5:155–161. https://doi.org/10.18576/ijtfst/050302

Meng L, Sun Y, Gong H, et al (2019) Research progress of the application of graphene-based materials in the treatment of water pollutants. Xinxing Tan Cailiao/New Carbon Materials 34:220–237. https://doi.org/10.1016/j.carbon.2019.06.092

Nisar A, Saeed M, Muneer M, et al (2021) Synthesis and characterization of ZnO decorated reduced graphene oxide (ZnO-rGO) and evaluation of its photocatalytic activity toward photodegradation of methylene blue. Environmental Science and Pollution Research. https://doi.org/10.1007/s11356-021-13520-6

Manigandan, K. Giribabu, R. Suresh, L. Vijayalakshmi, A. Stephen VN (2013) Cobalt Oxide Nanoparticles: Characterization and its Electrocatalytic Activity towards Nitrobenzene. Chemical Science Transactions 2:. https://doi.org/10.7598/cst2013.10

Rao KV, Sunandana CS (2008) Synthesis and characterization of Co3O4 nanoparticles. AIP Conference Proceedings 1003:97–99. https://doi.org/10.1063/1.2928996

Saeed M, Ahmad A, Boddula R, et al (2017) Ag@MnxOy: an effective catalyst for photo-degradation of rhodamine B dye. Environmental Chemistry Letters. https://doi.org/10.1007/s10311-017-0661-z

Saeed M, Ilyas M, Siddique M (2012) Oxidative degradation of phenol in aqueous medium catalyzed by lab prepared cobalt oxide. Journal of the Chemical Society of Pakistan 34:626–633

Song C, Wang LJ, Sun SM, et al (2020) Preparation of visible-light photocatalysts of Bi2O3/Bi embedded in porous carbon from Bi-based metal organic frameworks for highly efficient Rhodamine B removal from water. Xinxing Tan Cailiao/New Carbon Materials 35:609–618. https://doi.org/10.1016/S1872-5805(20)60513-3

Tang X, Feng Q, Huang J, et al (2018) Carbon-coated cobalt oxide porous spheres with improved kinetics and good structural stability for long-life lithium-ion batteries. Journal of Colloid and Interface Science 510:368–375. https://doi.org/10.1016/j.jcis.2017.09.086

Xu L, Meng L, Zhang X, et al (2019) Promoting Fe3+/Fe2+ cycling under visible light by synergistic interactions between P25 and small amount of Fenton reagents. Journal of Hazardous Materials 379:. https://doi.org/10.1016/j.jhazmat.2019.120795

Zhang L, Ghimire P, Phuriragpitikhon J, et al (2018) Facile formation of metallic bismuth/bismuth oxide heterojunction on porous carbon with enhanced photocatalytic activity. Journal of Colloid and Interface Science 513:82–91. https://doi.org/10.1016/j.jcis.2017.11.011

Zhao Z, Fan J, Deng X, Liu J (2019) One-step synthesis of phosphorus-doped g-C 3 N 4 /Co 3 O 4 quantum dots from vitamin B12 with enhanced visible-light photocatalytic activity for metronidazole degradation. Chemical Engineering Journal 360:1517–1529. https://doi.org/10.1016/j.cej.2018.10.239

Zhong YK, Zhou B, Zhang CJ, Wu D (2017) Effects of surface oxygen functional groups on activated carbon on the adsorption and photocatalytic degradation activities of a TiO2-AC hybrid for methylene blue and methylene orange. Xinxing Tan Cailiao/New Carbon Materials 32:460–466. https://doi.org/10.1016/j.carbon.2017.10.059

Figures

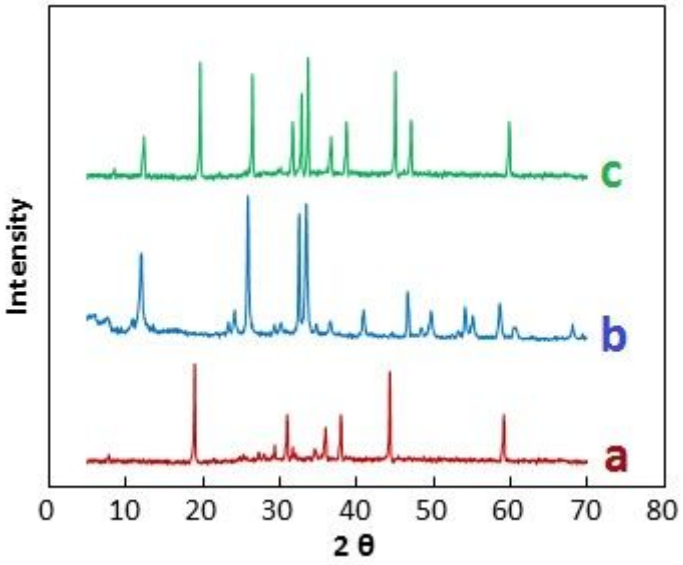

Figure 1

X-ray diffraction pattern of Co3O4 (a), Bi2O3 (b) and Co3O4-Bi2O3 (c)

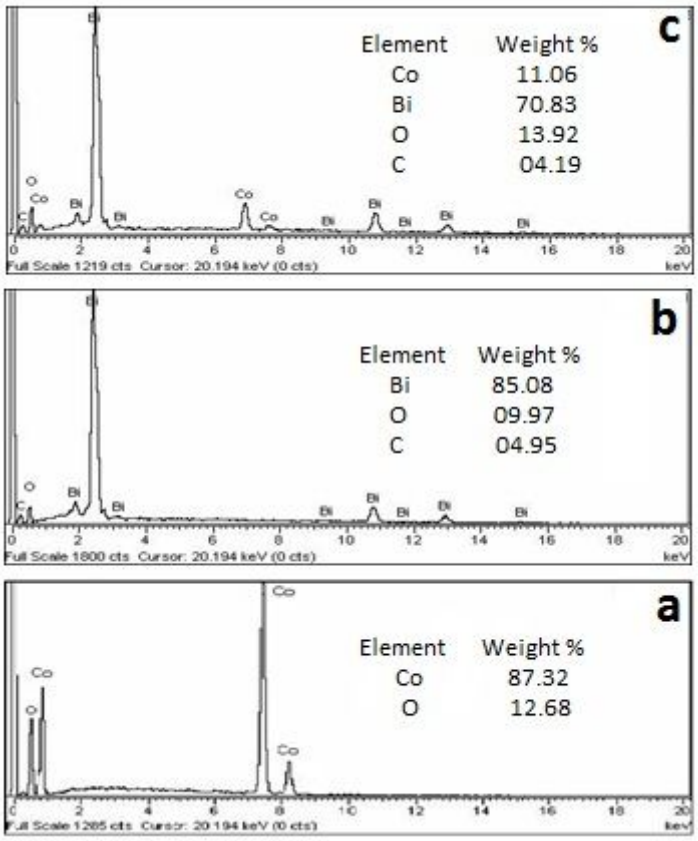

Figure 2

EDS analysis of Co3O4 (a), Bi2O3 (b) and Co3O4-Bi2O3 (c)

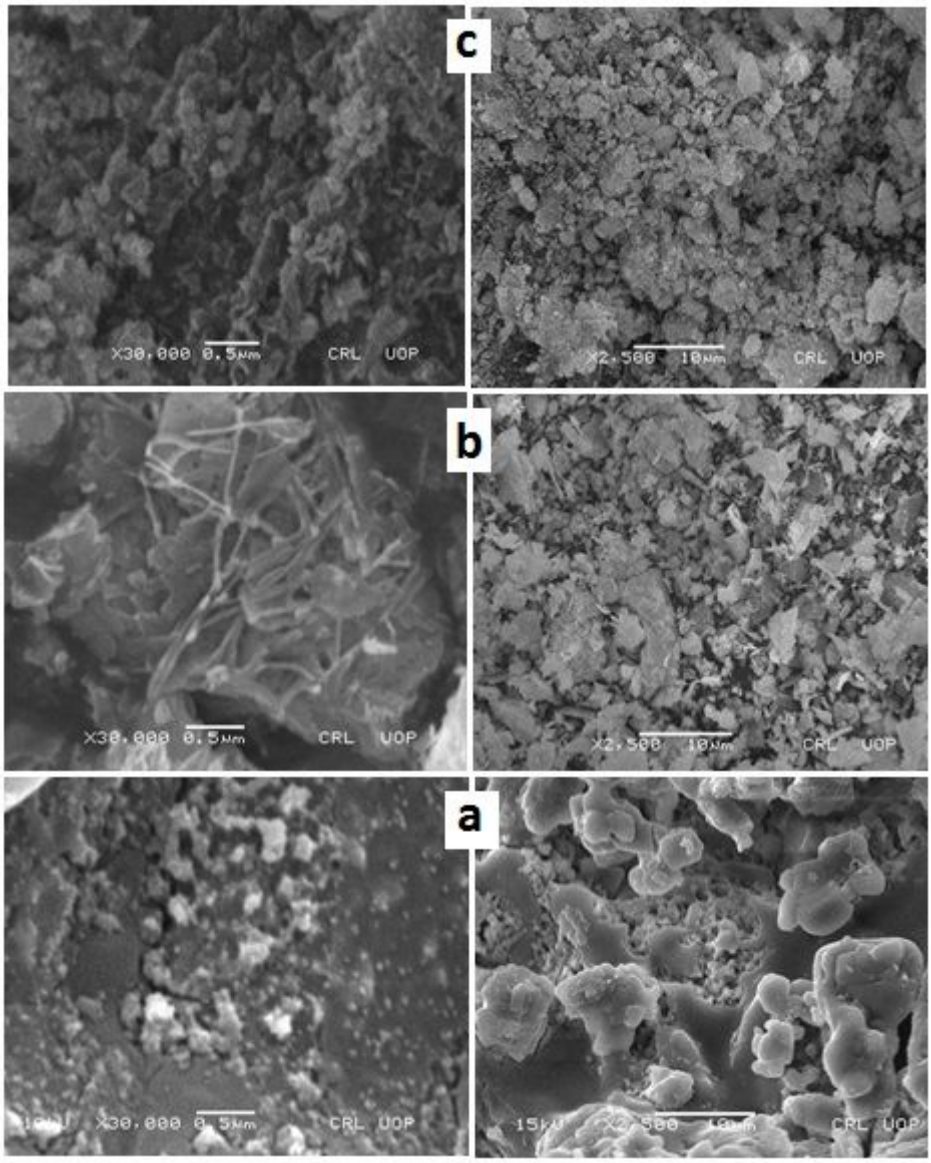

Figure 3

Scanning electron micrographs of Co3O4 (a), Bi2O3 (b) and Co3O4-Bi2O3 (c)

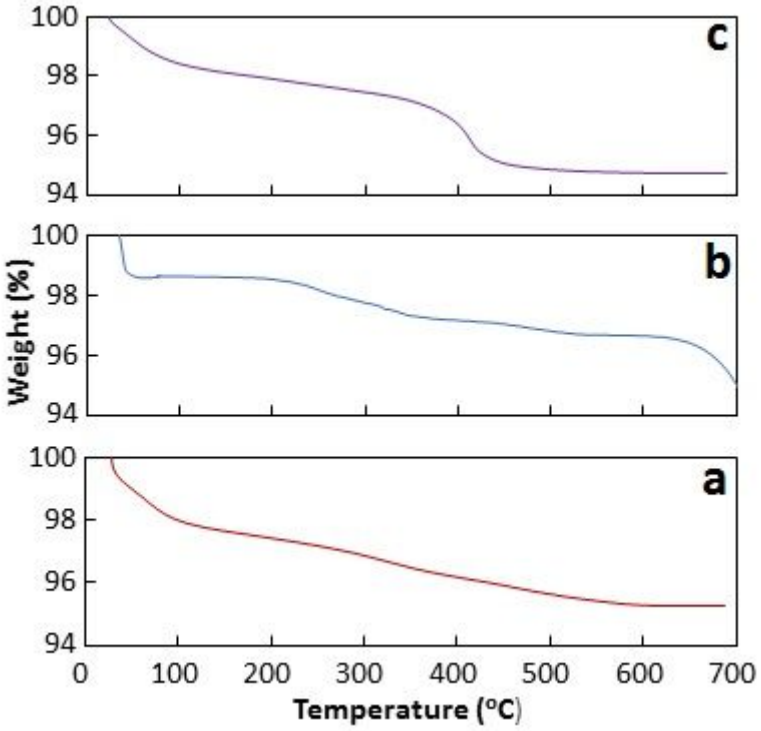

Figure 4

TGA analysis of Co3O4 (a), Bi2O3 (b) and Co3O4-Bi2O3 (c)

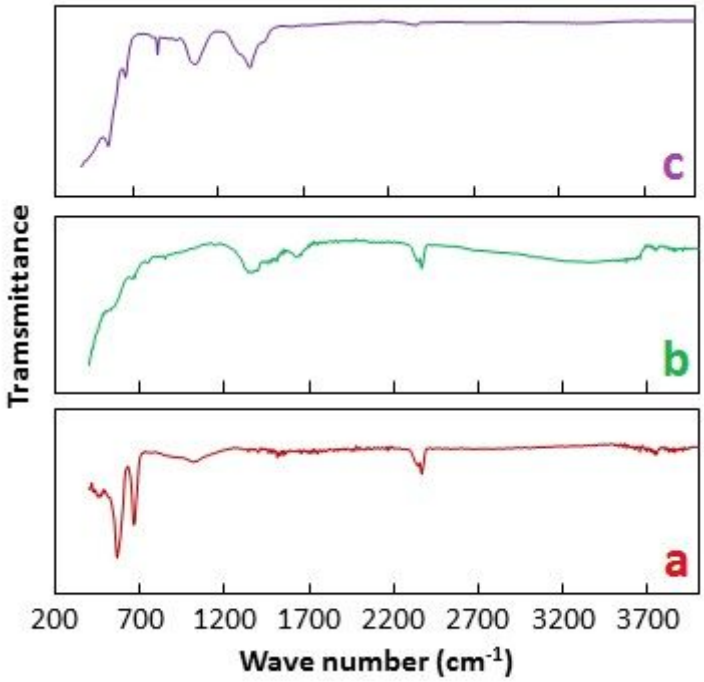

Figure 5

FTIR analysis of Co3O4 (a), Bi2O3 (b) and Co3O4-Bi2O3 (c)

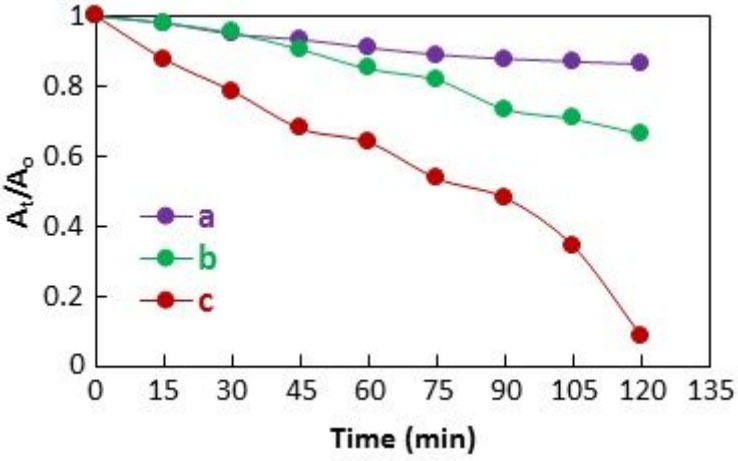

Figure 6

Photocatalytic activity of Co3O4 (a), Bi2O3 (b) and Co3O4-Bi2O3 (c) towards photodegradation of rhodamine B dye

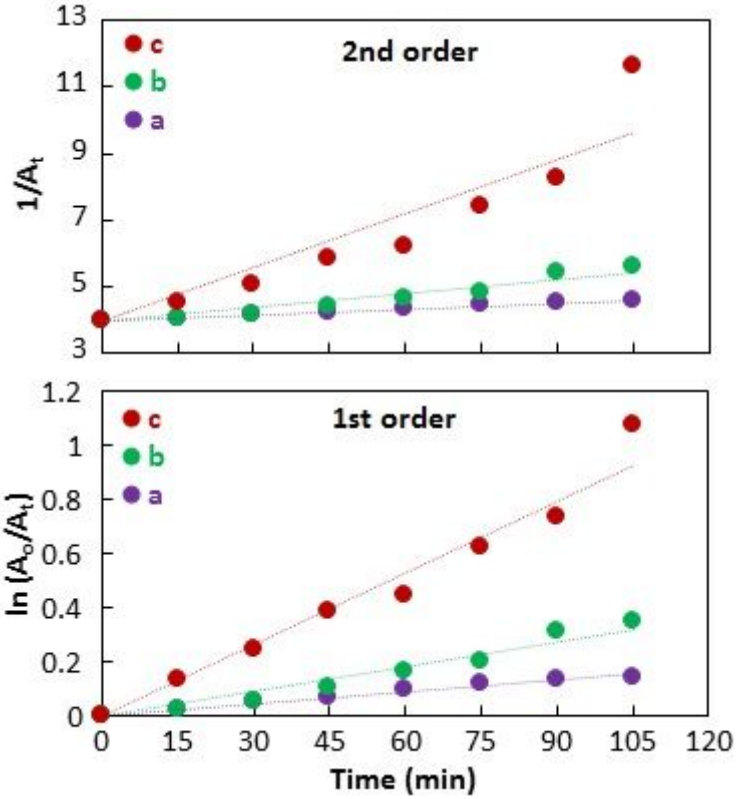

Figure 7

Kinetics treatment of experimental data with Co3O4 (a), Bi2O3 (b) and Co3O4-Bi2O3 (c)

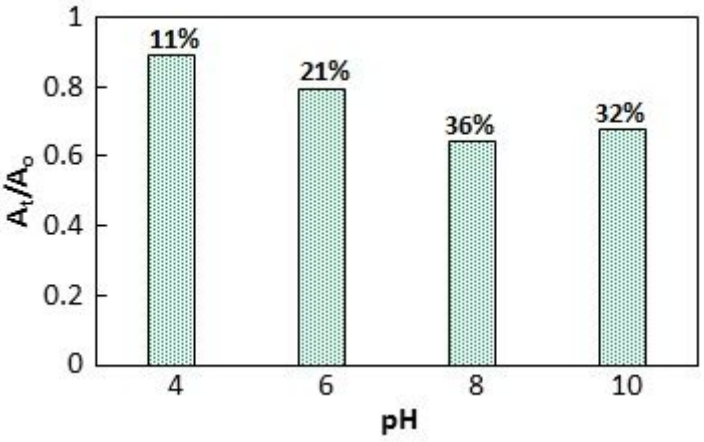

Figure 8

Effect of pH on catalytic activity of Co3O4-Bi2O3 towards photodegradation of rhodamine B

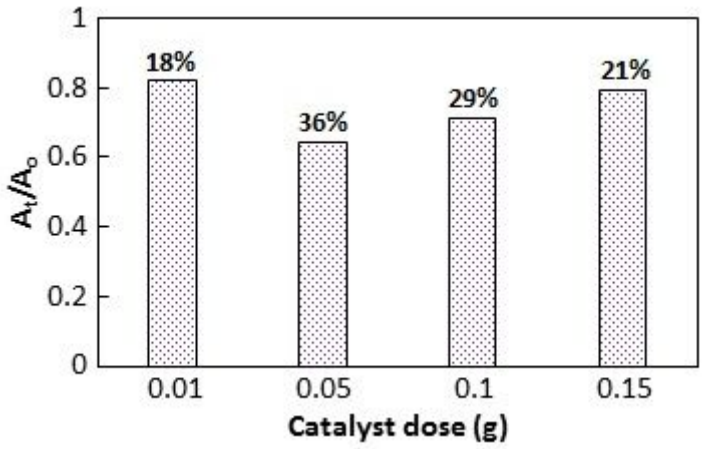

Figure 9

Effect of catalyst dose on catalytic activity of Co3O4-Bi2O3 towards photodegradation of rhodamine B

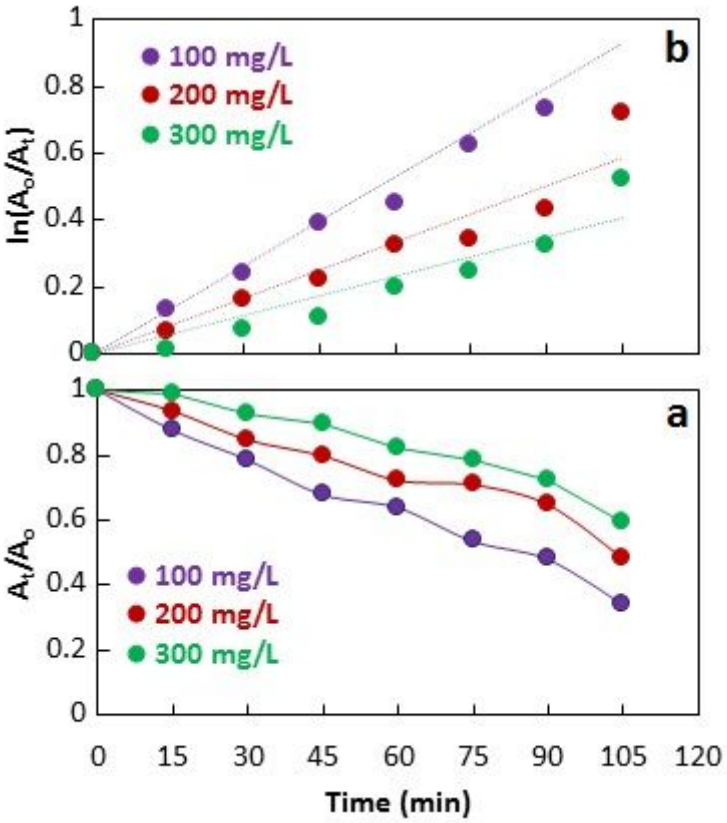

Figure 10

Effect of concentration of dye on catalytic activity of Co3O4-Bi2O3 towards photodegradation of rhodamine B